Energy and Buildings 158 (2018) 1368–1378

Contents lists available at ScienceDirect

Energy and Buildings

journal homepage: www.elsevier.com/locate/enbuild

Enhancing the performance of a zeolite 13X/$CaCl_2$–water adsorption cooling system by improving adsorber design and operation sequence

Ka Chung Chan [a,b,*], Chi Yan Tso [a,c], Chili Wu [b], Christopher Y.H. Chao [a]

[a] Department of Mechanical and Aerospace Engineering, The Hong Kong University of Science and Technology, Clear Water Bay, Kowloon, Hong Kong, China
[b] Fok Ying Tung Graduate School, The Hong Kong University of Science and Technology, Clear Water Bay, Kowloon, Hong Kong, China
[c] HKUST Jockey Club Institute for Advanced Study, The Hong Kong University of Science and Technology, Clear Water Bay, Kowloon, Hong Kong, China

ARTICLE INFO

Article history:
Received 29 May 2017
Received in revised form 9 October 2017
Accepted 19 November 2017
Available online 22 November 2017

Keywords:
Adsorption cooling systems
Composite adsorbent
Adsorber design
Operation sequence

ABSTRACT

In this study, a compact dual adsorber adsorption cooling system (ACS) prototype was built using the zeolite 13X/$CaCl_2$ composite adsorbent with water as the adsorbate. The adsorbers were constructed by directly coating the composite adsorbent on parallel flow finned heat exchangers to enhance the heat and mass transfer performance. The compactness of the ACS is of great concern for use in buildings, where space is always limited. Through a better adsorber design, the specific cooling power (SCP) is largely improved from 106 W/kg to 377 W/kg (256% improvement) under the same desorption temperature, 85 °C, and chilled water inlet temperature, 14 °C, even though the cooling water temperature is increased from 22 °C to 28 °C. Besides, four different operation sequences, namely basic cycle, mass recovery cycle, pre-heating & pre-cooling cycle, and mass recovery with pre-heating & pre-cooling cycle, were studied to optimize the system performance. It is found that performing the pre-heating & pre-cooling cycle can further increase the SCP to 401 W/kg. This promising result shows that the ACS has potential to be installed in buildings to achieve the goals of heating/cooling energy saving.

1. Introduction

Today, people spend a large portion of time in indoor environments. A huge amount of energy is consumed in order to provide a comfortable indoor environment. For example, 92% of the total electricity in Hong Kong was consumed by buildings at end-use level in 2014 [1]. Among different electricity end-uses, thermal systems contribute to a significant consumption of electricity in buildings, with 37% of electricity used to power space conditioning and refrigeration systems in buildings. Adsorption cooling systems (ACS) can be a sustainable alternative to the traditional vapor compression systems currently used in buildings, being an energy-efficient and environmentally friendly option for cooling and refrigeration. ACSs offer a number of distinct advantages as they do not require a compressor, which uses about 80% of the electricity consumed by a traditional air conditioner, while the solid non-toxic adsorbents and their corresponding refrigerants (e.g. water) of an ACS are environmentally friendly with zero ozone depletion potential and easy to handle in operation and maintenance. Thus, ACS has energy saving potential, featuring no moving parts and lower noise and vibration levels [2,3]. ACSs require a low-grade thermal energy source, possibly from solar energy or industrial waste heat, with minimal electricity required for other system components [4–7]. This could substantially reduce the dependence on fossil fuels, making the ACS a potential candidate for net zero energy building operation. In comparison with absorption cooling systems, the ACSs have no coolant pollution and no crystallization problems [8]. In comparison with a traditional vapor compression system, an ACS has the advantages of simple control, low initial investment and low noise [9]. A recent study compared the performance of a solar electrical vapor compression chiller, a solar thermal driven adsorption chiller and a hybrid solar electrical-thermal driven adsorption chiller [10]. The solar thermal system with the advanced flat plate solar collector has the shortest payback period of 7.6 years, while that of a solar electrical vapor compression chiller is more than 10 years. However, the bulkiness and heavy weight of an ACS presently limits its commercialization. The main challenge this technology faces is the low specific cooling power (SCP) that originates from the low adsorption capacity

* Corresponding author at: Department of Mechanical and Aerospace Engineering, Main Academic Building, The Hong Kong University of Science and Technology, Clear Water Bay, Kowloon, Hong Kong, China.
E-mail address: mekcchan@ust.hk (K.C. Chan).

https://doi.org/10.1016/j.enbuild.2017.11.040
0378-7788/

Nomenclature

c_p	Specific heat capacity, J/kg.K
$\dot{m}$	Mass flow rate, kg/s
COP	Coefficient of performance
SCP	Specific cooling power, W/kg
t_{cycle}	Cycle time, s
W	Weight of the composite adsorbent, kg
ω	Water uptake, kg/kg of adsorbent

Subscripts

chill	Chilled water
hot	Hot water

(i.e. 0.1–0.3 g/g), the low thermal conductivity of adsorbent particles (i.e. 0.1–0.4 W/mK) [11,12] and the low mass diffusivity of adsorbent-adsorbate pairs (i.e. 10^{-14}–10^{-8} m^2/s) [12,13].

To overcome these limitations, many researchers have devoted their work to develop different types of composite adsorbents for ACSs [14–17]. Hygroscopic salts, including lithium chloride (LiCl) and calcium chloride ($CaCl_2$), are often chosen and water is used as the adsorbate because hygroscopic salts have high affinity for water and water has a high latent heat of vaporization with no pollution implications. Chen et al. synthesized an attapulgite based LiCl composite adsorbent [18]. The water loading is as high as 0.44 kg/kg at 30 °C and 1500 Pa, and 0.31 kg/kg at 30 °C and 750 Pa. A composite adsorbent employing LiCl in silica gel was also developed [19]. The measured maximum water uptake was 0.39 kg/kg at 35 °C and 2621 Pa. Mobile Crystalline Material 41 (MCM-41) impregnated with $CaCl_2$ has achieved a reported coefficient of performance (COP) of 0.7 [14]. Daou et al. have developed a composite adsorbent by impregnating microporous silica gel with $CaCl_2$. They predicted that the SCP would be drastically increased by 2.87 times compared to the host silica gel [20]. Silica gel impregnated with $CaCl_2$, called selective water sorbent (SWS), shows an adsorption capacity of 0.7 g of water per gram of adsorbent. Systems using SWS have reported a COP of 0.6 and an SCP of 20 W/kg [15]. Saha et al. [16] investigated a two-bed adsorption chiller using a composite adsorbent called SWS-1L ($CaCl_2$ confined in silica gel). SWS-1L has a high water adsorption capacity, which shows a favorable characteristic as an adsorbent for ACSs [17]. Recently, a zeolite 13X/$CaCl_2$ composite adsorbent which has excellent adsorption related properties was developed by our research team [5]. The 13X/$CaCl_2$ composite adsorbent has much better performance than untreated zeolite 13X. A difference in equilibrium water uptake of 0.4 kg/kg between 25 °C and 75 °C at 870 Pa was recorded for the composite adsorbent impregnated in 40 wt% $CaCl_2$ solution. This was 420% of that of zeolite 13X and 233% of that of silica gel under the same condition. The ideal COP of an adsorber using the 13X/$CaCl_2$–water pair is 0.78 compared with 0.54 for the zeolite 13X-water pair. Simulation results suggest that the COP of a cooling system using the composite adsorbent would be 0.76, which is 81% better than a system using pure zeolite 13X. The SCP is also increased by 34% to 18.4 W/kg.

This composite adsorbent has also been studied experimentally [21]. The maximum SCP was found to be 106 W/kg in that study. Under the same operating condition, the SCP of the ACS using the composite adsorbent is approximately 30% higher than that of the same system using silica-gel as the adsorbent. Although a longer adsorption/desorption phase time (cycle time) is required for the ACS equipped with the composite adsorbent, it shows a better cooling performance than that of the silica gel adsorbent if a lower chilled water temperature, below 15 °C, is required. The SCP achieved is, however, too low for the ACSs to be commercialized. In addition to having a better adsorbent, a better adsorber bed design can also significantly improve the performance and reduce the footprint of an ACS. The combined heat and mass transfer during adsorption has a large effect on the COP and SCP of the system. The adsorbent has to be quickly heated and cooled such that more water

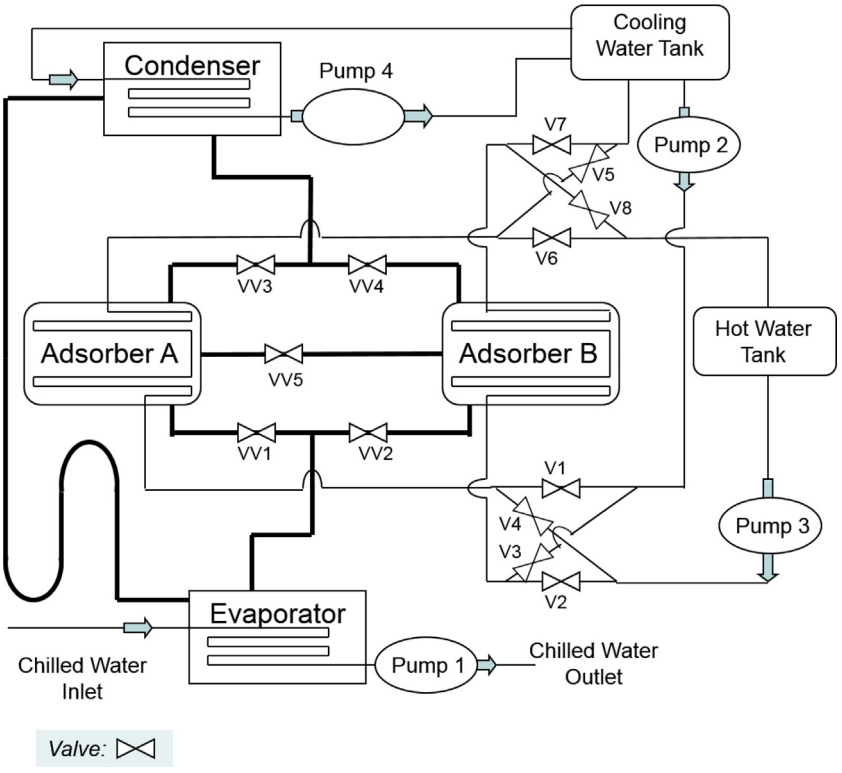

Fig. 1. Schematic diagram of the adsorption cooling system prototype. [Remark: Thinner lines: water pipeline for heating and cooling the adsorbers; Thicker lines: low pressure pipeline for water vapor or condensed water]

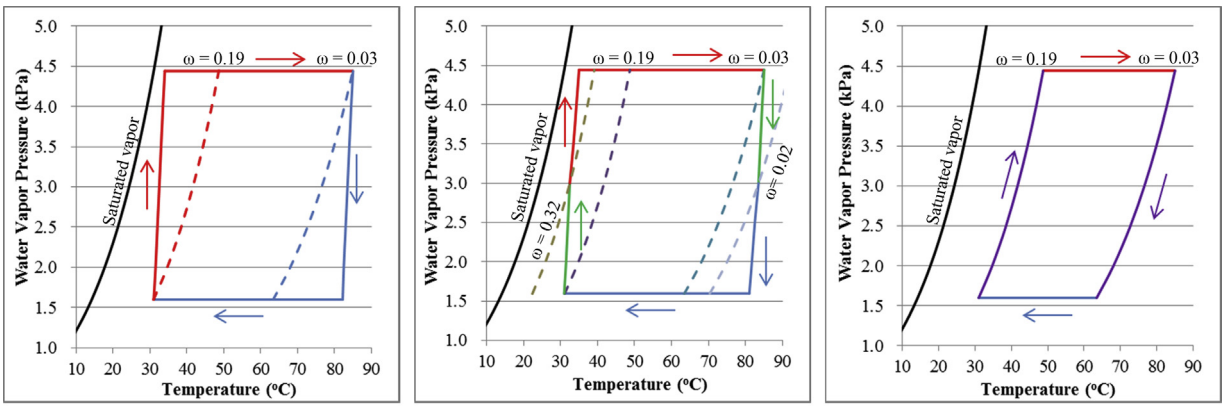

Fig. 2. P-T-W Diagrams of the studied operation cycles (a) Basic Cycle; (b) Mass recovery cycle; (c) Pre-heating & pre-cooling cycle. (For interpretation of the references to colour in this figure legend, the reader is referred to the web version of this article.) [Remarks: Red: desorption phase; Blue: adsorption phase; Green: Mass recovery phase; Purple: Pre-heating & pre-cooling phase]

vapor can be adsorbed to produce cooling within a shorter time. Adsorbents usually have low thermal conductivity [22]. Different adsorber designs have been tried to increase the overall thermal conductivity of the adsorber, including the use of extended surfaces like plate-fin heat exchangers [23], adsorbent-coated heat exchangers [24] and consolidated composite adsorbents [25]. An extended surface is not applicable for low pressure operation for zeolite-water, silica gel-water or activated carbon because of the Knudsen effect. The extended surface increases the thermal mass of the adsorber and lowers the COP and SCP of the system [26]. Coating adsorbent directly on the surface of a heat exchanger can reduce the thermal contact resistance between the adsorbent and the surface of the heat exchanger, but the low thermal conductivity of adsorbents limits the coating thickness to about 1 mm [27], limiting the COP and SCP of the system. Thus, the heat exchangers used for an adsorber have to be carefully selected to allow a good heat and mass transfer in the adsorbent bed.

Unlike a traditional vapor compression cooling system, the production of cooling in an ACS is intermittent. Thus, at least two adsorbers filled with adsorbents have to be used in order to produce a quasi-continuous cooling effect [28–30]. If the switching between the adsorption and desorption phase is not well controlled, a large amount of energy will be wasted, reducing the cooling production and efficiency [31,32]. Cycle time can significantly affect the COP and SCP of the system [4]. The solid adsorption system is an intermittent process so that the temperature and pressure of the components have to be changed for the adsorbers to adsorb and desorb adsorbate. Besides, heat and mass recovery are the processes that can improve system performance [3]. The stored regenerative heat in the desorbed adsorber is transferred to the saturated adsorber after adsorption by circulating the heat transfer fluid (HTF) between them. This can increase the system COP, since the heat left in the desorbed adsorber can be transferred to the adsorber that needs to be desorbed and the desorbed adsorber can thus cool faster [4]. In mass recovery, adsorbate is transferred between two adsorbers. It is reported that mass recovery can increase the SCP by up to 20% and COP by up to 100% [4].

This study aims to improve the performance of the ACS by: 1) Advanced composite adsorbent; 2) Directly coated adsorbers, and 3) Optimized operation sequence, in terms of SCP and COP. A dual bed adsorption cooling system prototype with directly

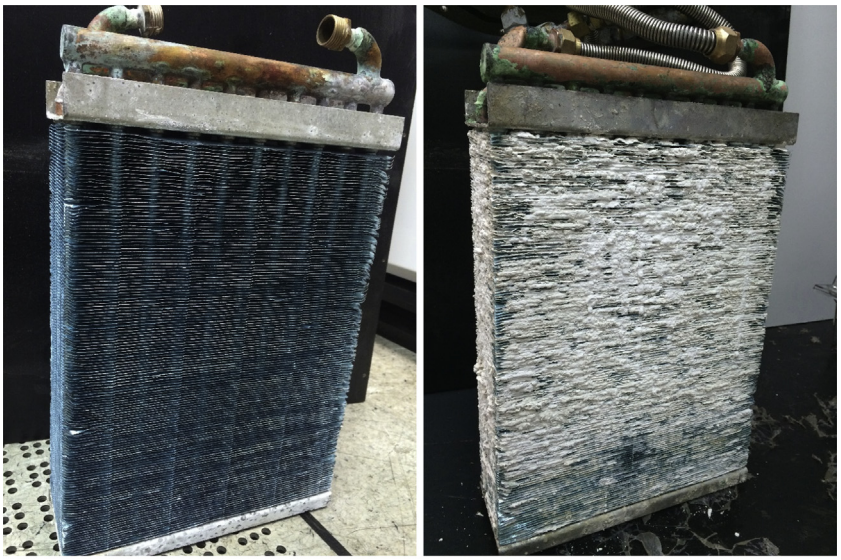

Fig. 3. Photographs of the heat exchanger (adsorbent bed). a) before and b) after coating with the composite adsorbent.

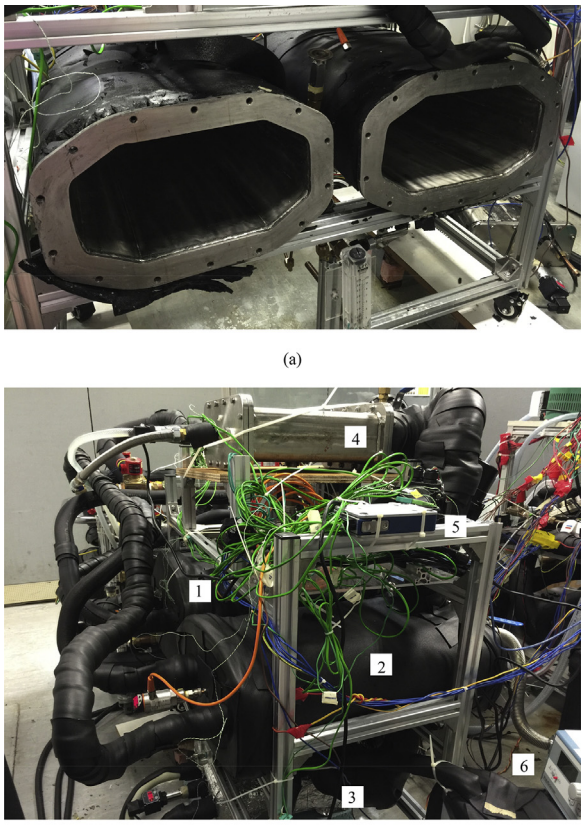

(a)

(b)

Fig. 4. A prototype of the ACS. a) vacuum chambers as adsorbers and b) overall view [Remarks: 1: Adsorber A; 2: Adsorber B; 3: chilled water tank (evaporator); 4: condenser; 5: DAQ device; 6: isothermal water circulator].

coated adsorbers was built. The zeolite 13X/$CaCl_2$ composite adsorbent was directly coated on a parallel flow heat exchanger with suitable fin pitch and hydrophilic coating. The prototype was investigated under various operating conditions, including the desorption temperature, phase time, cooling water inlet temperature and evaporating temperature. The effects of mass recovery, preheating and pre-cooling, and their combination were also studied.

2. Working principle of the adsorption cooling systems

ACSs can be compared to conventional vapor compression cooling systems for air conditioners, chillers or refrigerators in which the electric powered mechanical compressor is replaced by an adsorber. The system can be powered by a rather low driven temperature, e.g. waste heat or solar energy, which makes it attractive for saving electrical energy. Besides, the ACS can be operated with minimal moving parts; only solenoid vacuum valves are used. These result in low vibration, simple mechanics, high reliability and a very long life cycle [33,34]. As the adsorbent cannot be circulated [35], the system only produces cooling intermittently in the adsorption step. In order to provide a quasi-continuous cold production, a laboratory prototype of a double-bed ACS was designed and built, and its performance was analysed experimentally under different working conditions.

2.1. Basic operation phases of dual bed adsorption cooling systems

The basic operating cycle of the dual bed ACS consists of two phases, namely phase I and II. In phase I, adsorption takes place in Adsorber A, and desorption takes place in Adsorber B. In phase II, desorption takes in Adsorber A, and adsorption takes place in Adsorber B. A schematic diagram of a dual bed ACS is shown in Fig. 1. The thinner lines represent the water pipeline for heating and cooling the adsorbers, while the thicker lines represent the low pressure pipeline for water vapor or condensed water.

The system components and the pipeline for water vapor or condensed water are evacuated before operation. Water is then introduced into the evaporator and U-tube. The whole system is filled with low pressure water vapor. In phase I, valves VV1, VV4, V1, V2, V5 and V6 are opened. Adsorber A is connected to the evaporator. The water vapor is adsorbed by the composite adsorbent in the adsorber, maintaining a low pressure condition inside the evaporator, allowing the water to evaporate at a low temperature. Thermal energy in the chilled water is absorbed by the evaporated water. Adsorption heat is generated during the adsorption process in the adsorbent, and it has to be removed by providing the cooling water. Adsorber B is heated by the hot water, and water vapor is desorbed from the adsorbent. The desorbed water vapor is transferred to the condenser by the pressure difference between the adsorber and condenser. The water vapor is cooled and condensed in the condenser, and the heat released is transferred to the cooling water. The condensed water flows back to the evaporator via the U-tube connecting the condenser and evaporator, to complete the cycle [36,37]. In phase II, valves VV2, VV3, V3, V4, V7 and V8 are opened. By switching between the two phases in a dual bed ACS, a quasi-continuous cooling effect is produced.

Table 1
Standard operating conditions for the adsorption cooling system.

Parameters	Symbol	Value	Unit
Hot water inlet (desorption) temperature	$T_{hot,in}$	85	°C
Adsorber cooling water inlet temperature	$T_{cool,in}$	28	°C
Chilled water inlet temperature	$T_{chill,in}$	14	°C
Chilled water mass flow rate	$\dot{m}_{chill}$	5	kg/min
Hot water mass flow rate	$\dot{m}_{hot}$	14	kg/min
Cooling water mass flow rate	$\dot{m}_{cool}$	16	kg/min
Adsorption/desorption phase time	t_{phase}	8	mins
Mass recovery time	t_{mr}	22	seconds

Table 2
Varied operating conditions for the adsorption cooling system.

Parameters	Symbol	Value	Unit
Hot water inlet (desorption) temperature	$T_{hot,in}$	55, 65, 75, 95	°C
Adsorber cooling water inlet temperature	$T_{cool,in}$	19, 32, 43	°C
Chilled water inlet temperature	$T_{chill,in}$	8, 11, 17, 20	°C
Adsorption/desorption phase time	t_{phase}	2, 4, 12, 16, 20	mins

2.2. Mass recovery phase

At the end of the desorption phase, the pressure of the heated adsorber is higher than the cooled adsorber. The pressure of the cooled adsorber is equal to that of the evaporator, while the pressure of the heated adsorber is equal to that of the condenser. After that, the heated adsorber under high pressure needs to be cooled and depressurized while the cooled one needs to be heated and pressurized for the next phase. Before the next adsorption/desorption phase, mass recovery phase can be operated by opening VV5 to connect the two adsorbers together. Mass recovery should be conducted until the two adsorbers reach the same pressure. Then the valves are closed and the adsorbers are ready for the next phase.

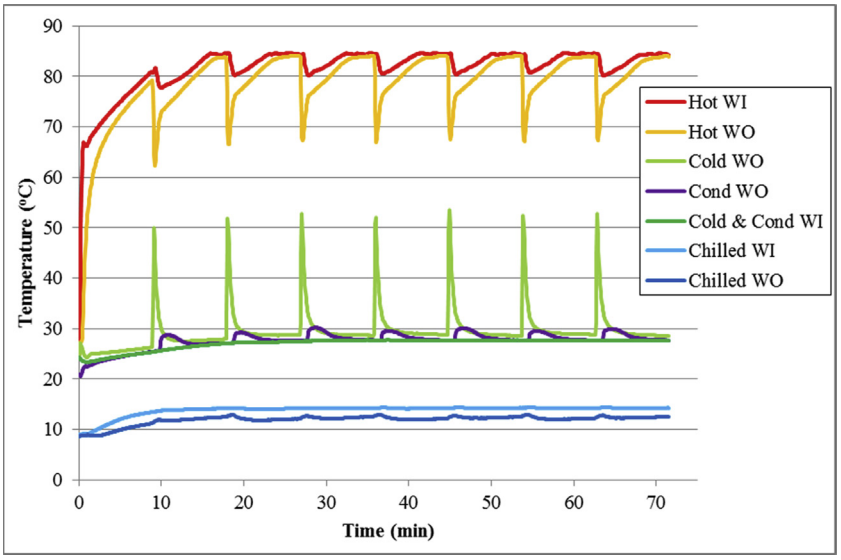

Fig. 5. Temperature profile of the heat transfer fluid during a typical experiment. [Remarks: WI: water in; WO: water out]

2.3. *Pre-heating & pre-cooling phase*

The pre-heating & pre-cooling phase is a pre-conditioning process. In the pre-heating & pre-cooling phase, the cooling water is connected to the desorber (the adsorber in the next phase), and the hot water is connected to the adsorber (the desorber in the next phase). When the pressures of the desorber and adsorber are nearly equal to the pressures of the condenser and evaporator respectively, the corresponding system components are connected. The P-T-W diagrams of basic, mass recovery and pre-heating & pre-cooling cycles are also presented in Fig. 2. The adsorbent-adsorbate pair shown in Fig. 2 is the composite adsorbent (Zeolite 13X/$CaCl_2$) and water.

3. Description of the adsorption cooling system prototype

The adsorber is the most important component of an ACS. Because of the poor thermal conductivity of the adsorbent materials commonly used in an ACS, the heat and mass transfer abilities of the adsorbers that affect the performance of the system should be considered carefully during the adsorber design. In this study, the composite adsorbents were directly coated on the fins of the heat exchangers (adsorbent beds). Fig. 3 shows photographs of a heat exchanger before and after coating with the composite adsorbent. The heat exchangers are parallel flow, made of copper tubes and aluminium fins, with a fin pitch of 1.8 mm and thickness of 0.115 mm. The dimensions of the heat exchangers are 264 mm (L) × 100 mm (L) × 420 mm (H). About 2 kg of composite adsorbent (zeolite 13X/$CaCl_2$) is coated on each heat exchanger. Thus, the thickness of the composite adsorbent coated on the fin surfaces is less than 1 mm for better heat transfer [27]. The heat exchangers also have a hydrophilic coating so the composite adsorbent can be adhered strongly to the metal surface. The coated heat exchangers (adsorbent beds) are put inside vacuum chambers, forming an adsorber. Photographs of the ACS prototype are shown in Fig. 4. All signals from thermocouples and pressure transducers were recorded by data acquisition (DAQ) devices from National Instrument. The thermocouple signals were recorded by NI 9213 16 channels thermocouple input module, while the pressure transducer signals were recorded by NI 9203 8 channels current input

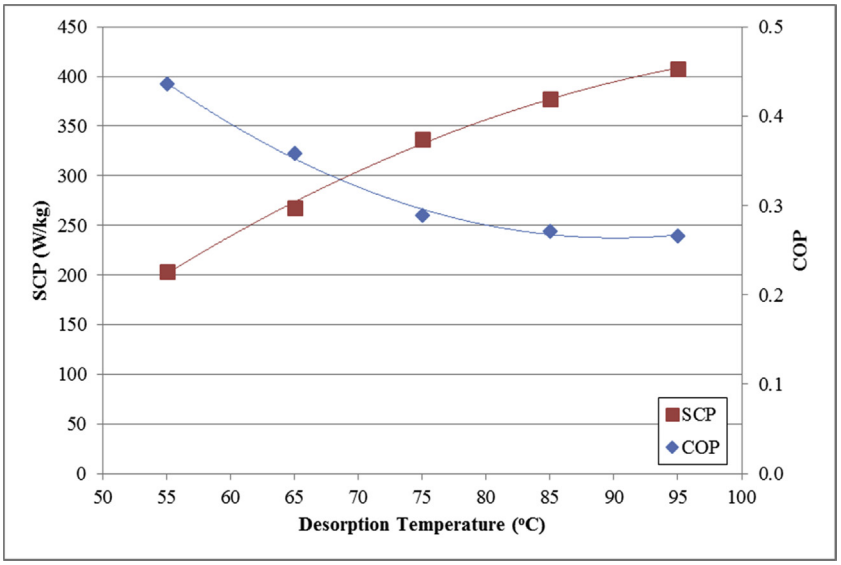

Fig. 6. Effect of desorption temperature on the SCP and COP.

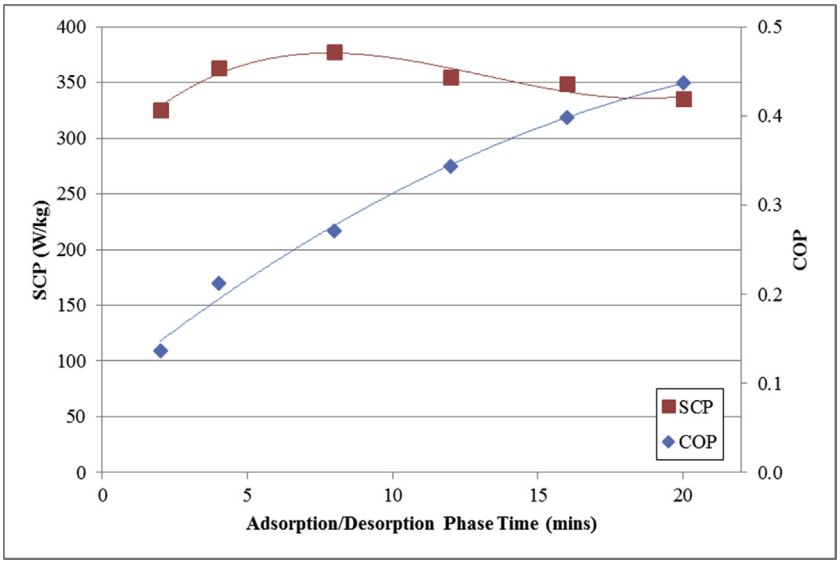

Fig. 7. Effect of adsorption/desorption phase time on the SCP and COP.

module, all connected to a computer. NI LabVIEW (version 9.0) was used to build a virtual DAQ program. Data was recorded every 5 s and stored in the computer's hard disk. Another LabVIEW program was built to control all valves and pumps through a NI SCXI-1160 16 channel general purpose relay module in an SCXI-1001 chassis. The program can control the valves individually or in a group, so the operation sequences of the ACS can be completed automatically.

In order to make a direct comparison with our previous work [21], the standard operating conditions for the ACS are the same and shown in Table 1, also for various conditions as listed in Table 2. The water flow rates are not varied and no flow restrictor is installed. This is because a higher flow rate will give a better heat transfer. Different operation sequences are listed in Table 3. Eq. (1) is used to calculate the SCP of the ACS:

$$SCP = \dot{m}_{chill} c_{p,water} \int_0^{t_{cycle}} (T_{chill,in} - T_{chill,out}) dt / W t_{cycle} \quad (1)$$

where $\dot{m}_{chill}$ is the mass flow rate of chilled water, $c_{p,water}$ is the specific heat capacity, W is the weight of the composite adsorbent

Table 3
Varied operating sequences for the adsorption cooling system. [I: Phase I; II: Phase II; MR: Mass Recovery; Pre-HC: Pre-heating & Pre-cooling]

Operating Sequences	
Basic Cycle	I → II → . . ..
Mass Recovery Cycle	I → MR → II → MR → I . . ..
Pre-heating & Pre-cooling Cycle	I → Pre-HC → II → Pre-HC → I . . ..
MR together with Pre-HC Cycle	I → MR & Pre-HC → II → MR & Pre-HC → I . . ..

(2 kg zeolite 13X/$CaCl_2$) and t_{cycle} is the cycle time. Eq. (2) is used to calculate the COP of the experimental prototype for different operating conditions. Specifically, this is referred to as the time-average COP:

$$COP = \int_0^{t_{cycle}} \left(\frac{\dot{m}_{chill} c_{p,water} (T_{chill,in} - T_{chill,out})}{\dot{m}_{hot} c_{p,water} (T_{hot,in} - T_{hot,out})} \right) dt / \int_0^{t_{cycle}} dt \quad (2)$$

where $\dot{m}_{hot}$ is the mass flow rate of hot water.

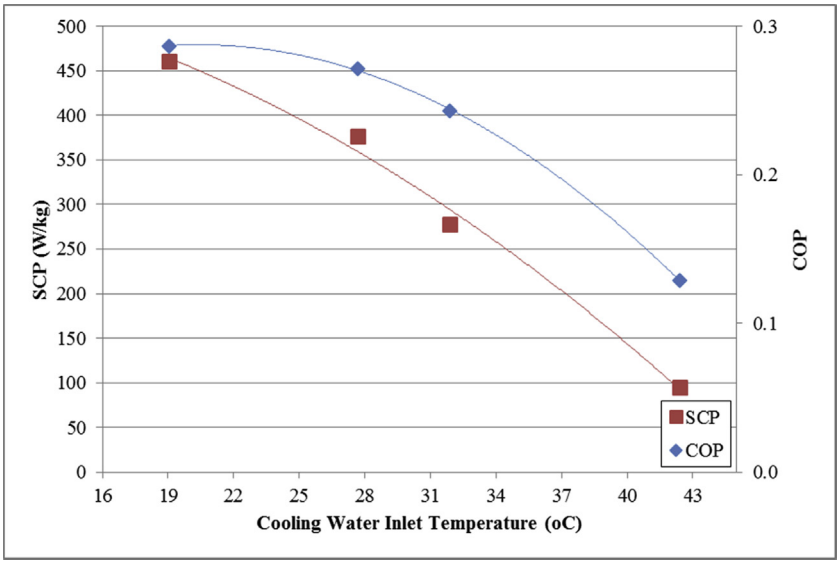

Fig. 8. Effect of cooling water inlet temperature on the SCP and COP.

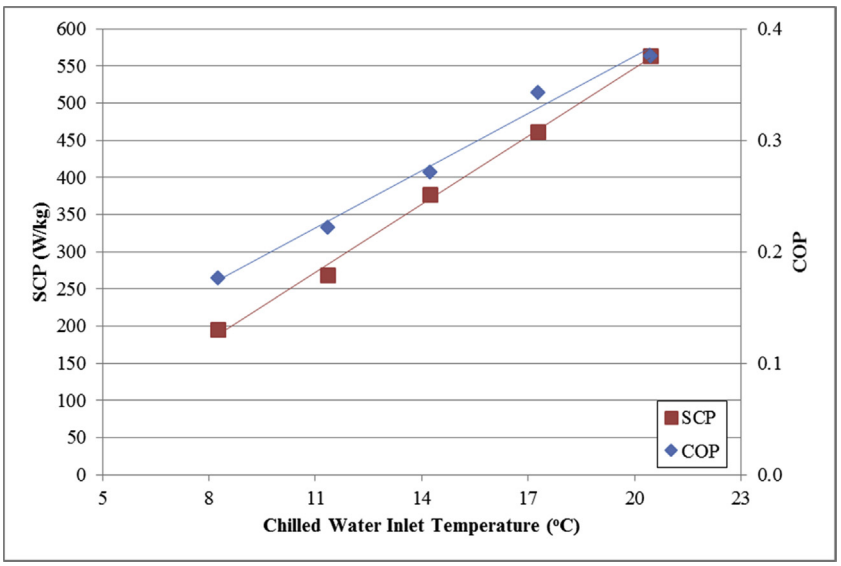

Fig. 9. Effect of chilled water inlet (evaporating) temperature on the SCP and COP.

4. Results and discussions

The performance of the prototype is investigated under various conditions. Since the thermal input power is obtained by the temperature difference between the inlet and outlet of the hot water tank, heat loss to the ambient environment is included in the calculation. The energy loss is mainly from the adsorbers, hot and cooling water tanks and piping system through which the heat transfer fluid (water) circulates. Fig. 5 shows the temperature profiles of the heat transfer fluid during a typical experiment. The data of the fourth cycle are used to calculate the SCP and COP to ensure that the system is under steady state operation.

4.1. Effect of desorption temperature

The desorption temperature is one of the major factors affecting the performance of ACSs. Fig. 6 shows the effect of the desorption temperatures on the SCP and COP. The water temperature in the hot water tank is controlled by a PID temperature controller. It is found that the SCP increases almost monotonically with the desorption temperature from 55 °C to 95 °C. Since the adsorbent is drier at the higher desorption temperature, this allows more water vapor to be adsorbed during the next adsorption process. A drier adsorbent can also adsorb water vapor at a faster rate according to the linear driving force model [38]. In other words, the higher the desorption temperature, the higher the SCP of the ACS.

However, the thermal energy used for desorption should be from solar energy or waste heat, from an energy saving point of view. A very high water temperature is hard to achieve. Therefore, standard hot water inlet temperature was selected to be 85 °C. Besides, solar energy and waste heat are free of charge, so the thermal COP values shown in this study are just for reference and comparison with other studies. SCP is indeed a very important parameter which indicates how large in size the ACS is along with the cooling power of the ACS.

4.2. Effect of adsorption/desorption phase time

Fig. 7 shows the effect of the adsorption/desorption phase time on the SCP and COP. All system parameters remained the same

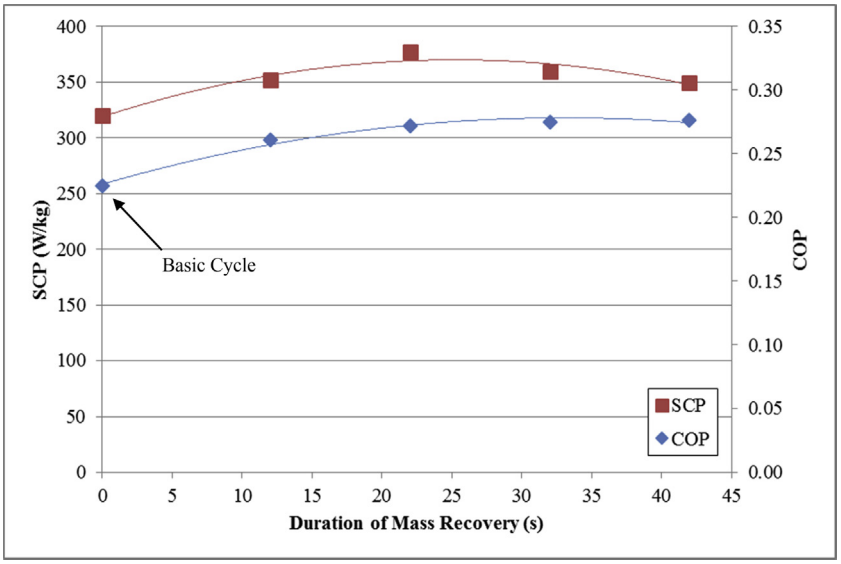

Fig. 10. Effect of duration of mass recovery phase on the SCP and COP.

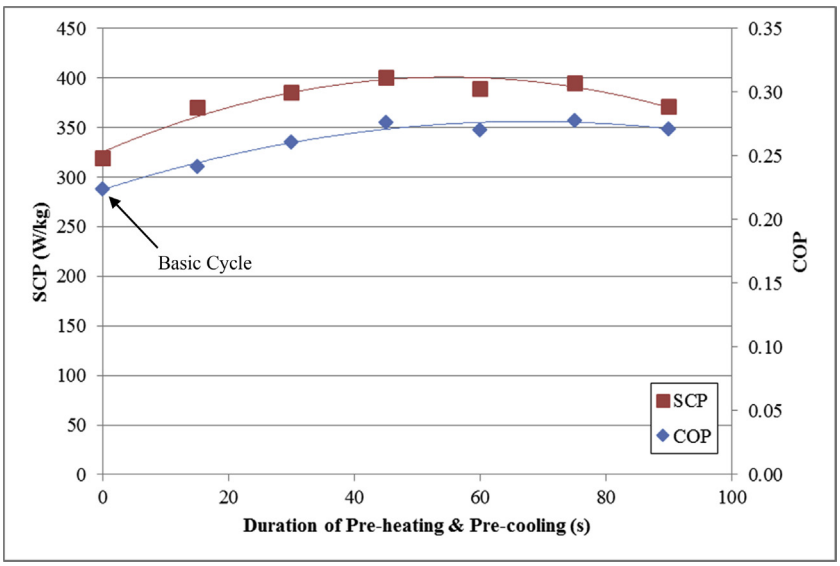

Fig. 11. Effect of duration of pre-heating & pre-cooling phase on the SCP and COP.

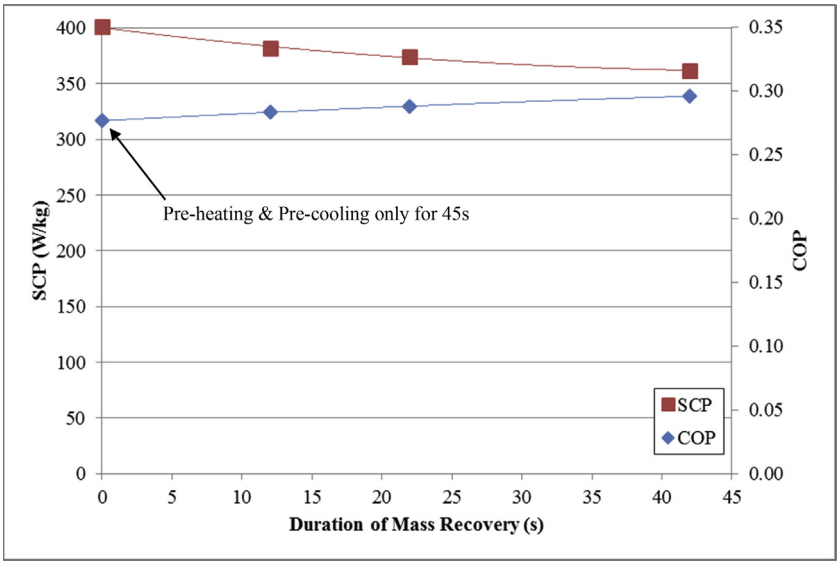

Fig. 12. Effect of duration of mass recovery together with pre-heating & pre-cooling phase on the SCP and COP (duration of pre-heating & pre-cooling was fixed at 45s).

Table 4
Comparisons among all the operating sequences.

Operating Sequences	SCP (W/kg)	ΔSCP	COP	ΔCOP
Previous study [21]	106	N.A.	0.16	N.A.
Basic Cycle (BC)	319	201%	0.22	40%
BC + Mass Recovery (MR for 22 s)	377	256%	0.27	70%
BC + Pre-heating & Pre-cooling Cycle (Pre-HC for 45 s)	401	278%	0.28	73%
BC + MR together with Pre-HC (MR for 42 s and Pre-HC for 45 s)	362	241%	0.30	85%

as shown in Table 1, except for the adsorption/desorption phase time. The phase time was set through the LabVIEW program. It is shown in Fig. 7 that 8 min is the best adsorption/desorption phase time for this ACS, because for shorter adsorption/desorption phase times, the desorption process is incomplete, leading to diminished adsorption capacity of adsorbents. As a result, the SCP is low at a shorter phase time. For longer phase times, the SCP decreases due to the rapid diminution of adsorption capacity of the adsorbents during the last few minutes. As a very thin layer of the composite adsorbent is formed on the fins of the heat exchanger compared to our previous study where the composite adsorbents were packed in between the copper circular fins (i.e. thickness of about 6 mm), the diffusion process of the water vapor through the composite adsorbents is much faster using the coating strategy presented in this study, leading to a significantly shorter adsorption/desorption phase time (i.e. the optimized adsorption/desorption phase time is about 8 min in this system, while it was 25 min in our previous study [21]).

Table 5
SCP comparison between this study and other experimental studies.

	Adsorbent – Adsorbate Working Pairs	Adsorber Packaging	Desorption Temperature (°C)	Chilled Water Inlet Temperature (°C)	Cooling Water Inlet Temperature (°C)	Cycle Time (minutes)	SCP (W/kg)
Zhang [39]	Zeolite 13X – water	Packed bed	310	10	25	131.5	25.7
Wang [4]	Activated carbon – methanol	Packed bed	96.8	9.9	29.6	40	151
Wang et al. [28]	Silica gel – water	Packed bed	85	12.2	29.4	10	115
Akahira et al. [31]	Silica gel – water	Packed bed	70	14	30	17	140
Wang et al. [40]	Silica gel – water	Packed bed	85	14	30.8	38	63.4
Liu et al. [41]	Silica-gel – water	Packed bed	85	14	30	17	52.8
Wang et al. [3]	Silica gel – water	Packed bed	86.8	21.1	30.9	32	102
Chang et al. [42]	Silica gel – water	Packed bed	80	14	30	26	72
Chen et al. [43]	Silica gel – water	Packed bed	85.1	11.7	30.9	28	132
Vasta et al. [44]	AQSOA-FAM-Z02 – water	Packed bed	90	13	28	7	260
Gong et al. [45]	Silica gel/LiCl – methanol	Packed bed	84.8	21.3	29.8	26	250
Freni et al. [46]	Silica gel/$Ca(NO_3)_2$ – water	Packed bed	95	15	30	10	400
Lu & Wang [47]	Silica gel/LiCl – methanol	Packed bed	86.6	9.2	31.4	16	95
Zhu et al. [48]	Silica gel – water	Packed bed	90	16	25	19	198
Thimmaiah et al. [49]	AQSOA FAM-Z02 – water	Directly coated	90	15	30	20	238
Vodianitskaia et al. [50]	Silica gel – water	Packed bed	80	15	30	80	68
Previous Study 1 [21]	Zeolite 13X/$CaCl_2$ – water	Packed bed	85	14	22	51	106
Previous Study 2 [37]	Silica gel – water	Packed bed	85	14	27	30.3	81.4
Present Study	Zeolite 13X/$CaCl_2$ – water	Directly coated	85	14	28	17.5	401

4.3. Effect of cooling water inlet temperature and chilled water inlet temperature

The cooling water inlet temperature is one of the decisive factors on the performance of ACSs because it influences not only the condensation process but also the adsorption process. The cooling water is used to cool down both the adsorber during adsorption and the condenser. If the temperature of the cooling water is high, both the performances of desorption and adsorption processes deteriorate, losing more refrigerating power. Fig. 8 shows the effect of the cooling water inlet temperature on the SCP and COP. The lower the cooling water inlet temperature, the higher the SCP and COP since more water vapor is adsorbed by the composite adsorbent at a lower temperature for a given cycle time. It is, however, desirable to use cooling water at room temperature in real practice. The cooling water inlet temperature averages 28 °C due to the operation of a water pump. Under this condition, the SCP is at about 376 W/kg with the COP about 0.27.

Fig. 9 shows the effect of the chilled water inlet temperature (evaporating temperature) on the SCP and COP. The chilled water inlet temperature is controlled by adjusting the set point of the isothermal water circulator shown in Fig. 4. Both SCP and COP rise with an increase in chilled water inlet (evaporating) temperatures. This is because the higher the chilled water inlet (evaporating) temperature, the higher the evaporating pressure is, leading to a larger amount of water vapor to be adsorbed by the composite adsorbent. The composite adsorbent can also adsorb more water under a higher water vapor pressure. As a result, the SCP and COP increase with the chilled water inlet (evaporating) temperature.

4.4. Effect of duration of mass recovery phase

Fig. 10 shows the SCP and COP of the ACS under different durations of mass recovery. The cycle with a 0 s mass recovery represents the basic cycle. The SCP and COP increase with the duration of mass recovery, and decrease when the duration is longer than 22 s. This is because the mass recovery is completed at about 22 s. A lengthy mass recovery process has no further benefit but unnecessarily increases the cycle time, reducing the SCP. The maximum SCP is 377 W/kg and is significantly increased by 255% from the previous prototype, where the highest SCP was 106 W/kg [21].

In the mass recovery process, the adsorbers are not connected to the evaporator and condenser. At the beginning of the mass recovery process, only VV5 is opened. The heated desorber is at a higher pressure condition while the cooled adsorber is at a lower pressure condition. By connecting the two adsorbers together, the desorbed water vapor flows from the high pressure heated desorber to the low pressure cooled adsorber. The mass recovery can further dry the desorber after desorption and reduce the internal pressure. The dryer adsorber can adsorb more water vapor in the next adsorption phase. This process leads the ACS to provide a better performance [29,30,32].

4.5. Effect of duration of pre-heating & pre-cooling phase

Besides mass recovery, pre-heating & pre-cooling can also improve the system performance. The improvement is shown in Fig. 11. The trend of increase in SCP and COP is similar to the effect of mass recovery. The maximum SCP is, however, further increased to 401 W/kg. After the adsorption phase, the internal pressure of the adsorber is low. If it were immediately connected to the condenser, water in the condenser would evaporate and flow back to the adsorber. This would increase the water uptake of the adsorbent in the adsorber and lower the system performance. A similar drawback would also appear on the desorption side. Hence, the pressure of the desorber has to be increased and that of the adsorber has to be decreased before connection to the condenser and evaporator.

4.6. Effect of duration of mass recovery together with pre-heating & pre-cooling phase

It has been shown that both mass recovery and pre-heating & pre-cooling can improve the system performance and their combination was also assessed to find out the possible enhancement. A set of experiments was conducted with the duration of pre-heating & pre-cooling fixed at 45 s. The result is shown in Fig. 12. It is found that performing mass recovery and pre-heating & pre-cooling together cannot further improve the SCP compared to pre-heating & pre-cooling only. The COP is, however, increased to 0.30 when the mass recovery is conducted for 42 s. This may be because the dried adsorber adsorbs the water vapor desorbed from the saturated adsorber. This not only reduces the available adsorption capacity in the next phase, but also reduces the amount of water to be desorbed. In other words, the cooling power of the system is reduced, but the energy required to desorb the adsorbers is

also reduced. This results in a lower SCP but higher COP. The SCP and COP of all the different cycles are summarized in Table 4.

5. Comparison with other and previous studies

The performance of the ACS prototype is also compared with other experimental studies in terms of SCP as shown in Table 5. In general, a higher desorption temperature [4,44,46,48,49] and a high chilled water inlet temperature [3,45] result in higher SCP. The composite adsorbents/advanced adsorbents also have better performance than traditional adsorbents [21,44–47,49]. The optimized performance of the ACS prototype in this study is close to that presented in [46]. However, the desorption temperature in their study is 95 °C, 10 °C higher than the present study. Thus, the SCP of the zeolite 13X/$CaCl_2$ ACS prototype would be higher than 400 W/kg. Besides, there are very few experimental results of the ACS employing a directly coated adsorber. The system using directly coated AQSOA FAM-Z02 built by Thimmaiah et al. shows a SCP of 238 W/kg.

6. Conclusions

In this study, a compact dual adsorber adsorption cooling system (ACS) prototype was built using the zeolite 13X/$CaCl_2$ composite adsorbent, with water as the adsorbate. The adsorbent was directly coated on the surface of the heat exchangers in the adsorbers. The heat transfer of the adsorbent is greatly improved by directly coating the heat exchangers. Thus, the SCP of the prototype is significantly improved from our previous study, where the adsorbent was packed between the copper circular fins. With the same desorption temperature, 85 °C, and chilled water inlet temperature, 14 °C, the SCP is increased from 106 W/kg to 377 W/kg, which is a 256% improvement, even though the cooling water temperature is increased from 22 °C to 28 °C. The COP is also improved from 0.16 to 0.27. This proves that coating the adsorbents on the fins of the heat exchanger substantially improved the cooling performance of the ACSs.

Four different operation cycles, namely basic cycle, mass recovery cycle, pre-heating & pre-cooling cycle and mass recovery together with pre-heating & pre-cooling cycle, were also investigated. Both mass recovery and pre-heating & pre-cooling cycles show improvement in the SCP and COP. The maximum SCP of 401 W/kg is achieved when pre-heating & pre-cooling is performed for 45 s. By performing mass recovery together with pre-heating & pre-cooling, the SCP is not improved as much as with performing pre-heating & pre-cooling, but the COP is maximized to be 0.30. From these results, it is confirmed the performance of the ACS can be substantially enhanced by the improved adsorber design and operation optimization. With more development, the ACS can be installed in buildings to reduce the energy consumption for cooling, working towards net zero energy buildings.

Acknowledgements

Funding sources for this research are provided by the Hong Kong Research Grant Council via General Research Fund account16201114; Guangzhou Science and Technology Program via account 2016201604030056, Science and Technology Program of Nansha District via account 2015KF029 and Postdoc Station at Guangzhou Nansha via account 180852.

References

[1] Hong Kong Energy End-Use Data 2016, Electrical & Mechanical Services Department, Hong Kong, 2016.
[2] B.B. Saha, S. Koyama, T. Kashiwagi, A. Akisawa, K.C. Ng, H.T. Chua, Waste heat driven dual-mode multi-stage, multi-bed regenerative adsorption system, Int. J. Refrig. 26 (2003) 749–757.
[3] R.Z. Wang, R.G. Oliveira, Adsorption refrigeration — an efficient way to make good use of waste heat and solar energy, Prog. Energy Combust. Sci. 32 (2006) 424–458.
[4] R.Z. Wang, Performance improvement of adsorption cooling by heat and mass recovery operation, Int. J. Refrig. 24 (2001) 602–611.
[5] K.C. Chan, C.Y.H. Chao, G.N. Sze-To, K.S. Hui, Performance predictions for a new zeolite 13X/$CaCl_2$ composite adsorbent for adsorption cooling systems, Int. J. Heat Mass Transfer 55 (2012) 3214–3224.
[6] C.Y. Tso, C.Y.H. Chao, Activated carbon, silica-gel and calcium chloride composite adsorbents for energy efficient solar adsorption cooling and dehumidification systems, Int. J. Refrig. 35 (2012) 1626–1638.
[7] C.Y. Tso, C.Y.H. Chao, S.C. Fu, Performance analysis of a waste heat driven activated carbon based composite adsorbent −water adsorption chiller using simulation model, Int. J. Heat Mass Transfer 55 (2013) 7596–7610.
[8] K.R. Ullah, R. Saiur, H.W. Ping, R.K. Akikur, N.H. Shuvo, A review of solar thermal refrigeration and cooling methods, Renew. Sustain. Energy Rev. 24 (2013) 499–513.
[9] K. Wang, J.Y. Wu, R.Z. Wang, L.W. Wang, Composite adsorbent of $CaCl_2$ and expanded graphite for adsorption ice maker on fishing boats, Int. J. Refrig. 29 (2006) 199–210.
[10] E.G. Papoutsis, I.P. Koronaki, V.D. Papaefthimiou, Numerical simulation and parametric study of different types of solar cooling systems under Mediterranean climatic conditions, Energy Build. 138 (2017) 601–611.
[11] F. Poyelle, J.J. Guilleminot, F. Meunier, Experimental tests and predictive model of an adsorptive air conditioning unit, Ind. Eng. Chem. Res. 38 (1) (1999) 298–309.
[12] Z. Tamainot-Telto, R.E. Critoph, Monolithic carbon for sorption refrigeration and heat pump applications, Appl. Therm. Eng. 21 (1) (2001) 37–52.
[13] A. Sharafian, M. Bahrami, Adsorbate uptake and mass diffusivity of working pairs in adsorption cooling systems, Int. J. Heat Mass Transfer 59 (2013) 262–271.
[14] M. Tokarev, L. Gordeeva, V. Romannikov, I. Glaznev, Y.I. Aristov, New composite sorbent $CaCl_2$ in mesopores for sorption cooling/heating, Int. J. Therm. Sci. 41 (2002) 470–474.
[15] G. Restuccia, A. Freni, S. Vasta, Y.I. Aristov, Selective water sorbent for solid sorption chiller: experimental results and modeling, Int. J. Refrig. 27 (2004) 284–293.
[16] B.B. Saha, A. Chakraborty, S. Koyama, Y.I. Aristov, A new generation cooling device employing CaCl2-in-silica gel-water system, Int. J. Heat Mass Transfer 52 (2009) 516–524.
[17] Y.I. Aristov, New family of solid sorbents for adsorptive cooling: material scientist approach, J. Eng. Thermophys. 16 (2) (2007) 63–72.
[18] H.J. Chen, Q. Cui, Y. Tang, X.J. Chen, H.Q. Yao, Attapulgite based LiCl composite adsorbents for cooling and air conditioning applications, Appl. Therm. Eng. 28 (2008) 2187–2193.
[19] L.X. Gong, R.Z. Wang, Z.Z. Xia, C.J. Chen, Adsorption equilibrium of water on a composite adsorbent employing lithium chloride in silica gel, J. Chem. Eng. Data 55 (2010) 2920–2923.
[20] K. Daou, R.Z. Wang, Z.Z. Xia, Development of a new synthesized adsorbent for refrigeration and air conditioning applications, Appl. Therm. Eng. 26 (2006) 56–65.
[21] C.Y. Tso, K.C. Chan, C.Y.H. Chao, C.L. Wu, Experimental performance analysis on an adsorption cooling system using zeolite 13X/$CaCl_2$ adsorbent with various operation sequences, Int. J. Heat Mass Transfer 85 (2015) 343–355.
[22] M.B. Jakubinek, B.Z. Zhan, M.A. White, Temperature-dependent thermal conductivity of powdered zeolite NaX, Microporous Mesoporous Mater. 103 (2007) 108–112.
[23] R.D. Boer, S.F. Smeding, R.J.H. Grisel, Development and testing of a sorbent filled heat exchanger for use in compact solid sorption cooling systems, in: Proceedings of International Sorption Heat Pump Conference, Denver, USA, 2005.
[24] A.M.W. Wojcik, J.C. Jansen, T. Maschmeyer, Regarding pressure in the adsorber of an adsorption heat pump with thin synthesized zeolite layers on heat exchangers, Microporous Mesoporous Mater. 43 (2001) 313–317.
[25] Z. Tamainot-Telto, R.E. Critoph, Adsorption refrigerator using monolithic carbon-ammonia pair, Int. J. Refrig. 20 (1997) 146–155.
[26] F. Meunier, Solid sorption heat powered cycles for cooling and heating pumping application, Appl. Therm. Eng. 18 (1998) 715–729.
[27] G. Restuccia, G. Cacciola, Performance of adsorption systems for ambient heating and air conditioning, Int. J. Refrig. 22 (1) (1999) 18–26.
[28] X. Wang, H.T. Chua, K.C. Ng, Experimental investigation of silica gel–water adsorption chillers with and without a passive heat recovery scheme, Int. J. Refrig. 28 (2005) 756–765.
[29] K.C. Ng, X. Wang, Y.S. Lim, B.B. Saha, A. Chakarborty, S. Koyama, A. Akisawac, T. Kashiwagi, Experimental study on performance improvement of a four-bed adsorption chiller by using heat and mass recovery, Int. J. Heat Mass Transfer 49 (2006) 3343–3348.
[30] K.C. Leong, Y. Liu, System performance of a combined heat and mass recovery adsorption cooling cycle: a parametric study, Int. J. Heat Mass Transfer 49 (2006) 2703–2711.
[31] A. Akahira, K.C. Alam, Y. Hamamoto, A. Akisawa, T. Kashiwagi, Experimental investigation of mass recovery adsorption refrigeration cycle, Int. J. Refrig. 28 (2005) 565–572.
[32] X. Wang, K.C. Ng, A. Chakarborty, B.B. Saha, How heat and mass recovery strategies impact the performance of adsorption desalination plant: theory and experiments, Heat Transfer Eng. 28 (2) (2007) 147–153.

[33] W.S. Loh, I.I. El-Sharkawy, K.C. Ng, B.B. Saha, Adsorption cooling cycles for alternative adsorbent/adsorbate pairs working at partial vacuum and pressurized conditions, App. Therm. Eng. 29 (4) (2009) 793–798.
[34] K. Thu, Y.D. Kim, B.J. Xi, A. Ismail, K.C. Ng, Thermophysical properties of novel zeolite materials for sorption cycles, App. Mech. Mater. 388 (2013) 116–122.
[35] A.B. Ismail, A. Li, K. Thu, K.C. Ng, W. Chun, On the thermodynamics of refrigerant + heterogeneous solid surfaces adsorption, Langmuir 29 (47) (2013) 14494–14502.
[36] H.T. Chua, K.C. Ng, W. Wang, C. Yap, X.L. Wang, Transient modeling of a two-bed silica gel–water adsorption chiller, Int. J. Heat Mass Transfer 47 (4) (2004) 659–669.
[37] K.C. Chan, C.Y. Tso, C.Y.H. Chao, C.L. Wu, Experiment verified simulation study of the operating sequences on the performance of adsorption cooling systems, Build. Simul. 8 (3) (2015) 255–269.
[38] A. Sakoda, M. Suzuki, Fundamental study on solar powered adsorption cooling system, J. Chem. Eng. Jpn. 17 (1) (1984) 52–57.
[39] L.Z. Zhang, Design and testing of an automobile waste heat adsorption cooling system, Appl. Therm. Eng. 20 (2000) 103–114.
[40] D.C. Wang, J.Y. Wu, Z.Z. Xia, H. Zhai, R.Z. Wang, W.D. Dou, Study of a novel silica gel −water adsorption chiller, part II experimental study, Int. J. Refrig. 28 (2005) 1084–1091.
[41] Y.L. Liu, R.Z. Wang, Z.Z. Xia, Experimental performance of a silica gel–water adsorption chiller, Appl. Therm. Eng. 25 (2005) 359–375.
[42] W.S. Chang, C.C. Wang, C.C. Shieh, Design and performance of a solar-powered heating and cooling system using silica-gel/water adsorption chiller, Appl. Therm. Eng. 29 (2009) 2100–2105.
[43] C.J. Chen, R.Z. Wang, Z.Z. Xia, J.K. Kiplagat, Z.S. Lu, Study on a compact silica gel −water adsorption chiller without vacuum valves: design and experimental study, Appl. Energy 87 (2010) 2673–2681.
[44] S. Vasta, A. Freni, A. Sapienza, F. Costa, G. Restuccia, Development and lab-test of a mobile adsorption air-conditioner, Int. J. Refrig. 35 (2012) 701–708.
[45] L.X. Gong, R.Z. Wang, Z.Z. Xia, Z.S. Lu, Experimental study on an adsorption chiller employing lithium chloride in silica gel and methanol, Int. J. Refrig. 35 (2012) 1950–1957.
[46] A. Freni, A. Sapienza, I.S. Glaznev, Y.I. Aristov, G. Restuccia, Experimental testing of a lab-scale adsorption chiller using a novel selective water sorbent silica modified by calcium nitrate, Int. J. Refrig. 35 (2012) 518–524.
[47] Z.S. Lu, R.Z. Wang, Study of the new composite adsorbent of salt LiCl/silica gel–methanol used in an innovative adsorption cooling machine driven by low temperature heat source, Renew. Energy 63 (2014) 445–451.
[48] L.Q. Zhu, Z.W. Gong, B.X. Ou, C.L. Wu, Performance analysis of four types of adsorbent beds in a double-adsorber adsorption refrigerator, Procedia Eng. 121 (2015) 129–137.
[49] P.C. Thimmaiah, A. Sharafian, M. Rouhani, W. Huttema, M. Bahrami, Evaluation of low-pressure flooded evaporator performance for adsorption chillers, Energy 122 (2017) 144–158.
[50] P.J. Vodianitskaia, J.J. Soares, H. Melo, J.M. Gurgel, Experimental chiller with silica gel: adsorption kinetics analysis and performance evaluation, Energy Convers. Manage. 132 (2017) 172–179.